11th International Conference on Fracture Mechanics of Concrete and Concrete Structures
FraMCoS-11
J. M. Chandra Kishen, A. Ramaswamy, S. Ray and R. Vidyasagar (Eds)
https://doi.org/10.21012/FC11.092333

EFFECT OF DILATION ANGLE AND ECCENTRICITY PARAMETERS ON THE BEHAVIOUR OF RC SHEAR WALLS

CH. HYMAVATHI ANNAPOORNA*, AND G. APPA RAO†

* Research Scholar, Department of Civil Engineering
Indian Institute of Technology Madras,Chennai,India
e-mail:ce20d065@smail.iitm.ac.in

† Professor, Department of Civil Engineering
Indian Institute of Technology Madras,Chennai,India
e-mail: garao@iitm.ac.in

Key words: Concrete Damage Plasticity, Dilation angle, Eccentricity, Shear Walls and Viscosity Parameter

Abstract. Strong finite element (FE) modeling can capture the nonlinear behavior of RC structures. In this study, Finite Element Analysis (FEA) tool, ABAQUS has been adopted to model the reinforced concrete shear wall with defined boundary conditions. The Concrete Damage Plasticity (CDP) model includes the tension and compression behavior of concrete. The linear behaviour is defined by modulus of elasticity and Poisson's ratio. The non-linear behaviour in compression and tension is incorporated through the yield stress and crushing strain, yield stress and cracking strain respectively. To incorporate the effect of complex stress state, the ratio of biaxial compressive strength-to-uniaxial compressive strength, the ratio of the second stress invariant on the tensile meridian-to-the compressive meridian, viscosity parameter, eccentricity and dilation angle need to be clearly prescribed. Previous studies show that viscosity μ, dilation angle ψ and eccentricity e_c are the important parameters affecting the output to a great extent. As there is a huge disparity in the value of these parameters that need to be incorporated into the model, the present study attempts to demonstrate the influence of viscosity and dilation angle along with eccentricity in capturing the strength and the failure mechanism of the shear wall. Study shows that a dilation angle of 46^o with eccentricity 1.0 could able to capture the diagonal tensile failure of the shear wall considered.

1 INTRODUCTION

Reinforced concrete shear walls are the common lateral-load resisting systems in structures. They are observed in most of the reinforced concrete structures subjected to earthquake forces. Depending upon their height-to-length ratio they are classified as squat and slender walls. Squat walls with a height-to-length ratio of less than two are commonly observed in nuclear power plants and low-rise buildings [1]. Failure in such squat walls is usually dominated by shear behavior. Depending upon the horizontal and vertical reinforcement ratios, wall dimensions, and axial load ratio, squat walls can exhibit Diagonal compression, diagonal tension and sliding shear mode of failure [2–4].

The design philosophy of shear walls is to suppress the brittle mode of failure such that a good amount of energy dissipation is observed before final failure. This can be achieved by strengthening the wall's shear carrying capacity higher than the flexure capacity to ensure the yielding of the vertical reinforcement [5]. Thus predicting the flexure and shear carrying capacity of the wall sections is very much important in understanding the behavior and mode of failure.

Finite element modeling is an advanced tool to study the behavior of RC structures. FEM analysis of RC structures includes defining the material model for concrete and steel. Material models used should be capable enough to exhibit the behaviour in both the elastic and inelastic regions to capture the complete behaviour of the structure. The inelastic properties of Steel can be modeled using plasticity model accurately whereas concrete, complex material needs sophisticated models to represent its behavior in non-linear regime [6]. Concrete Damage Plasticity is a continuum damage based model developed for concrete to represent the elastic behavior in cyclic, monotonic and dynamic loading conditions [7]. The CDP model assumes tensile cracking and concrete crushing as the main failure mechanism of concrete [6]. A damage parameter ranging between 0 to 1.0 can be incorporated for compression and tension to include stiffness or strength degradation.

CDP model primarily requires three different sets of data including the plasticity parameters, uniaxial compressive behaviour and uniaxial tensile behaviour. The uniaxial tensile and uniaxial compressive behaviour represents the stress vs strain behaviour under uniaxial loading condition. In addition to this the plasticity parameters are assigned to define the failure surface of the concrete. These plasticity parameters include dilation angle ψ, ratio of biaxial stress to uniaxial stress in compression $\frac{f_{bo}}{f_{co}}$, eccentricity e_c, the ratio of second stress invariant on tensile and compressive meridian k_c and viscosity parameter μ [8].

Literature showed that the plasticity parameters dilation angle ψ, eccentricity e_c and viscosity parameterμ affect the response of the model. Most of the work in the past showed a dilation angle of 5^{o} -55^{o}, eccentricity between 0.1 to 1.0 used for the RC structures. None of the work could be able to define a clear conclusion on the viscosity parameter to be used in the modeling. Thus, the present study focuses on the influence of these parameters on the strength and failure mode prediction of the RC squat shear wall.

2. ANALYTICAL MODELLING

A finite element model for a wall of thickness of 100 mm, length of 1180 mm, and height of 1200 mm is developed in the commercially available software ABAQUS standard. A vertical reinforcement ratio of 0.99% is incorporated using a total 24 number of 8 mm diameter bars with a spacing of 100 mm in two layers [9].

2.1Modelling scheme

Wall and the reinforcement are modeled as deformable homogenous and isotropic bodies. To reduce the stiffness of the system, wall is modeled using eight-node brick elements with Linear reduced integration (C3D8R) element type. As the axial effects are predominant in reinforcement, modeled using a two-node linear truss element (T3D2). The strain in reinforcement is assumed to be the same as in that of concrete and a perfect bond is assumed between the concrete and reinforcement in the model. To confirm the perfect bond, the interaction between concrete and reinforcement is defined as an embedded constraint in the interaction module of ABAQUS. A mesh size of 50 mm x 50mm x 50mm is confirmed to give better results and thus a 50 mm mesh is assumed for further parametric studies in the present work.

2.2 Constitutive Relation

The behaviour of the deformable bodies is analyzed using the constitutive relation in elastic and plastic regions. As concrete and steel are assumed to be homogeneous and isotropic, the Modulus of elasticity and Poisson's ratio are suffice to capture the elastic behaviour. Plastic behaviour is modelled using the Concrete Damage Plasticity (CDP) model for concrete and plasticity model for the reinforcement.

CDP model in ABAQUS is defined using the parameters of plasticity, uniaxial compressive behaviour, and tensile behaviour. The uniaxial behaviour in compression is shown in figure 1 obtained using the modified Kent and Park model by Paulay [10] using equation [1- 2]. As the wall is not provided with any confined reinforcement, k factor is set to 1.0 and boundary reinforcement factor ρ_s to zero.

Between A and B: $\epsilon_c \leqslant 0.002$

$$f_c = k\, f_c'[\frac{2\varepsilon_c}{0.002\, k} - (\frac{\varepsilon_c}{0.002\, k})^2] \qquad [1]$$

Between B and C: $\varepsilon_c \geq \varepsilon_o$

$$f_c = k\, f_c'[1 - Z_m(\varepsilon_c - 0.002k)^2] \qquad [2]$$

Where,

$$Z_m = [\frac{0.5}{\frac{3 + 0.29 f_c'}{145 f_c' - 1000} + 0.75\rho_s\sqrt{\frac{b"}{s_h}} - 0.002k}]$$

$$\rho_s = \frac{2(b" + d")A_s}{b"d"s_h}$$

$$k = 1 + \frac{\rho_s f_{yh}}{f_c'}$$

Where ϵ_c the strain at corresponding stress f_c, k is the confining factor, ϵ_o is the strain in concrete at concrete compressive strength, f_c'(29.2 MPa).

The tensile behaviour of concrete shown in figure 2, as modeled using equations [3- 4] by Belarbi and Hsu [11] and the tensile strength of concrete is taken as $0.33\sqrt{f_c'}$. A linear behaviour is adopted upto tensile strength and the post-peak is used as per equation 4

If $\varepsilon_t \leq \varepsilon_{cr}$

$$\sigma_t = E_c \varepsilon_t \qquad [3]$$

If $\varepsilon_r > \varepsilon_{cr}$

$$\sigma_t = f_t \left(\frac{\varepsilon_{cr}}{\varepsilon_t}\right)^{0.4} \qquad [4]$$

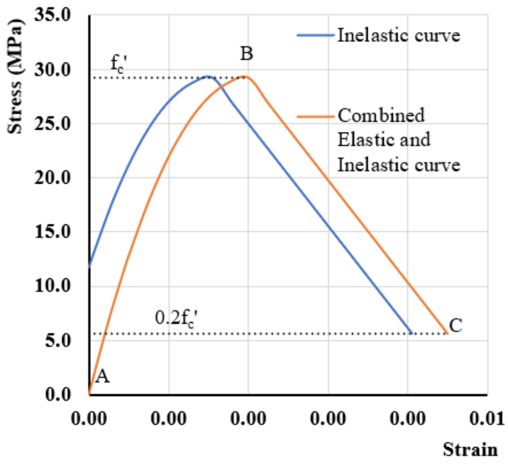

Figure 1 Behaviour of concrete in uniaxial compression

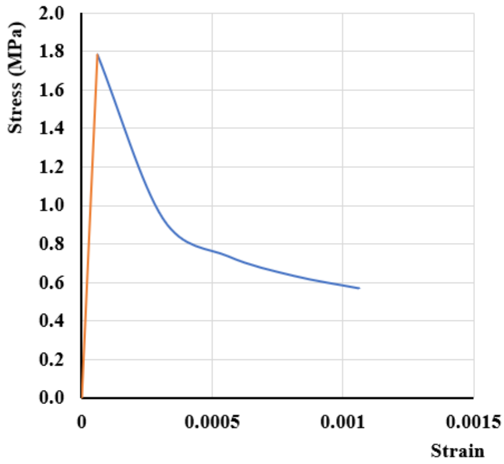

Figure 2 Behaviour of concrete in uniaxial tensión

where E_c is the modulus of elasticity of concrete (2.88×10^4MPa), ϵ_t is tensile strain corresponding to tensile stress σ_t, ϵ_{cr} is the cracking strain at the maximum tensile strength of concrete f_t.

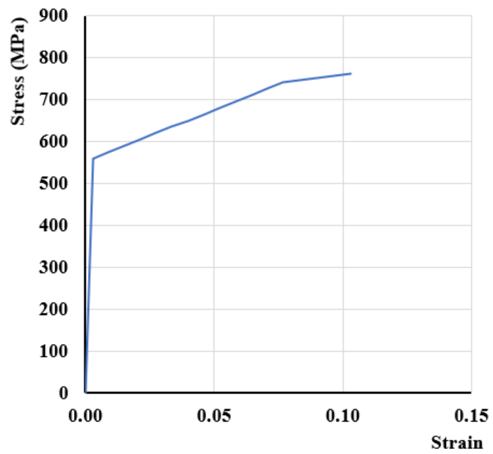

Figure 3 Stress-Strain relation for steel reinforcement

A bilinear model for reinforcement, in figure 3, is assumed with yeild strength of f_y 560 MPa and ultimate strength f_u of 762 MPa. Modulus of elasticity and Posission's ratio of steel are 2×10^5 MPa and 0.3 respectively. The strain in steel at yield ϵ_{sv} is 0.002 and strain at ultimate ϵ_{su} 0.103.

2.3 CDP Plasticity Parameters

Along with uniaxial behaviour of concrete in compression and tension, plasticity parameters like dilation angle ψ, ratio of biaxial stress to uniaxial stress in compression $\frac{f_{bo}}{f_{co}}$, eccentricity e_c, the ratio of second stress invariant on tensile and compressive meridian k_c is defined to capture multi-axial behaviour of concrete. Dilation angle and eccentricity parameters are used in developing the flow potential function. Viscosity parameter in plasticity definition explains the behaviour of concrete when transforming from uncracked to cracked concrete[8].

The values of 1.16 and 0.667 have been adopted for biaxial stress-to-uniaxial stress in compression, $\frac{f_{bo}}{f_{co}}$ and ratio of second stress invariant on tensile and compressive meridian k_c respectively. A parametric study to define the optimum dilation angle ψ, eccentricity e_c, and viscosity parameter μ has been carried out.

2.4 Solver and Step Definition

An implicit solver is chosen for its reliability and the step is defined as static general. The axial and the lateral loads are defined in two different steps. An axial load of 260 kN is defined as pressure on the top end of the wall and lateral load is applied through displacement at all nodes at top-face in the load module. Bottom end of the wall is restricted to translate in all three directions by defining the boundary condition in the step definitions.

3. PARAMETERS

A total of 12 models have been developed by considering a range of dilation angle ψ, eccentricity e_c and viscosity parameters to study the effect on the strength. 46°, 52° and 56° are considered to study the effect of dilation angle and the influence of viscosity parameter is also observed by changing the parameter in the range 5E-5, 0.001, 0.003, 0.004 and 0.005. Finally, the influence of eccentricity e_c is observed by changing its values from 1.0 to 0.1.

4. RESULTS AND DISCUSSION

The pushover curve from finite element models is compared with the experimental curve in terms of the influence of dilation angle ψ, viscosity parameter μ. The eccentricity e_c value is obtained by comparing the pushover curves for these models. The eccentricity value 1.0 is maintained while accessing the effect of viscosity e_c and dilation angle ψ.

Firstly, the dilation angle has been set to 56° and different models are analysed by changing the viscosity parameter ranging from 5E-5 to 0.005. It has been observed, from figure 4, that the maximum load changes with viscosity parameter. To confirm the effect of viscosity parameter, models have been analysed with dilation angle 52° with viscosity range 0.001, 0.003, 0.004 and 0.005 and for models with dilation angle 46° a viscosity parameter values 0.004 and 0.005 are used. From figures 5- 6, it can be confirmed that an increase in viscosity parameter increases the maximum load.

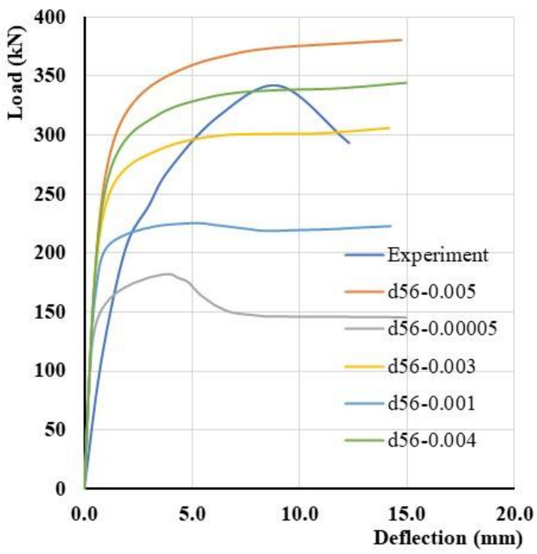

Figure 4 Load vs. deflection curve for dilation angle 56^0 with varying viscosity parameter

From figures 4-6, it can be inferred that a value of 0.004 and 0.005 for viscosity parameter gave satisfactory results. To further optimize the models which can predict the behaviour with a minimal error, a comparison between the dilation angle 46°, 52° and 56° with viscosity parameters of 0.004 and 0.005 are shown in figures 7-8. It is observed that the maximum load is also influenced by the dilation angle. The dilation angle shows a positive relation with the maximum load. For viscosity parameter valuses 0.005 and 0.004, there has been an increase in the load carrying capacity as the dilation angle increases.

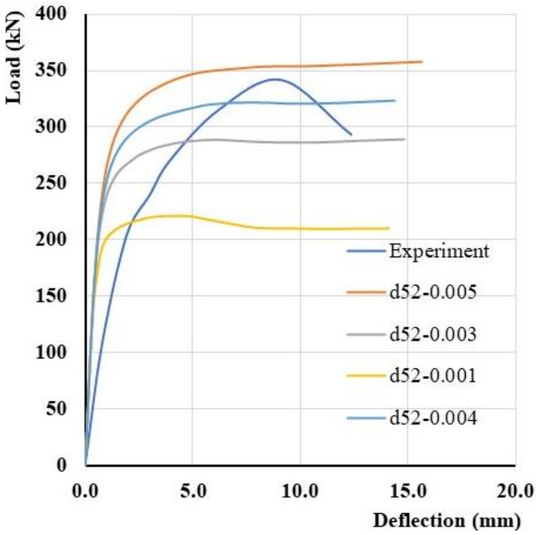

Figure 5 Load vs. deflection response for dilation angle 52° with varying viscosity parameter

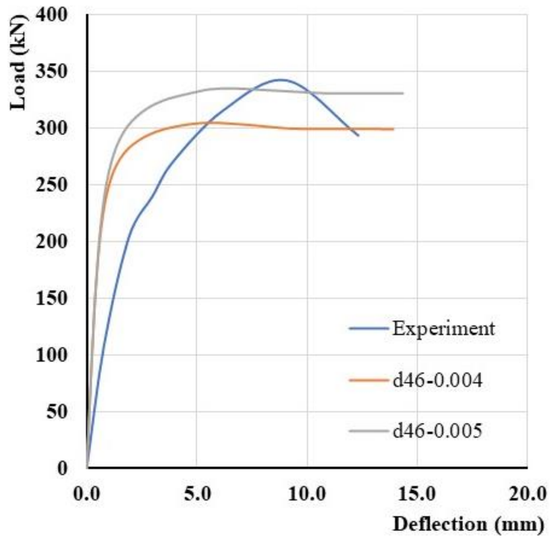

Figure 6 Load vs. deflection response for dilation angle 46° with varying viscosity parameter

From figures 7-8, it has been observed that the load vs. deflection response monotonically increases with the dilation angles 56° and 52° for the viscosity parameters 0.005 and 0.004. For the dilation angle 46°, a drop in the load vs. deflection response has been observed after the peak for viscosity parameter values of 0.005 and 0.004 as well. From figures 7-8, it can be observed that viscosity parameter also affects the load-deflection response in the non-linear region.

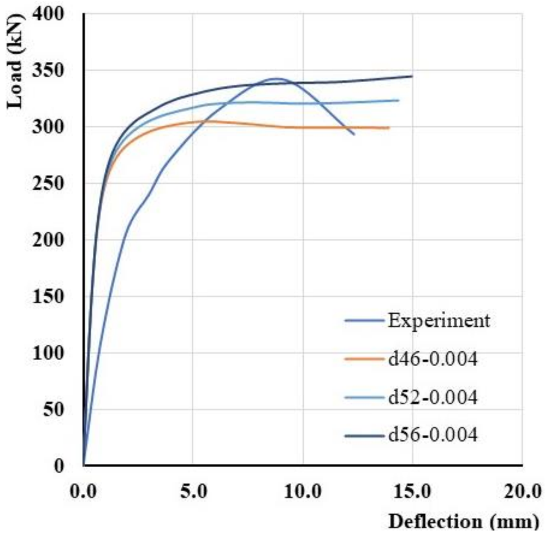

Figure 7 Load vs. deflection curve for viscosity parameter 0.004 and varying dilation angle

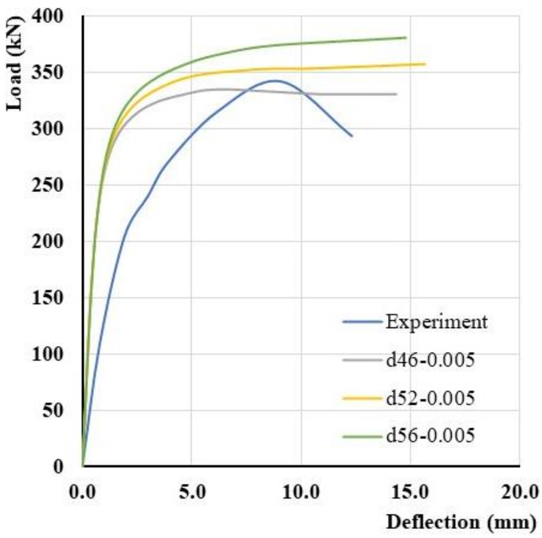

Figure 8 Load vs. deflection response for viscosity parameter 0.005 and varying dilation angle

To confirm the effect of eccentricity e_c two models with e_c 1.0 and 0.1 with constant dilation angle (46°) and viscosity parameter

(0.005) have been analyzed. There is a drop in the maximum load corresponding to eccentricity e_c (0.1) when compared to with eccentricity e_c value 1.0 as shown in figure 9.

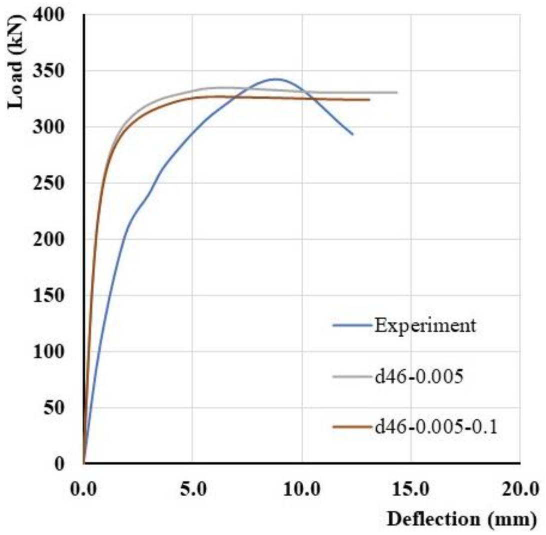

Figure 9 Load vs. deflection curve for viscosity parameter 0.005, dilation angle 46° and varying eccentricity

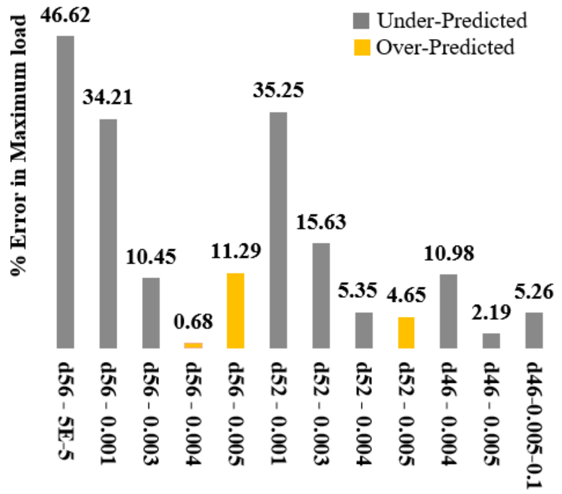

Figure 10 Percentage errors in the maximum load compared to experimental máximum

The performance of the plasticity parameter has been studied by comparing the experimental maximum with the analytical maximum. The experimental maximum is observed to be 342kN and the percentage errors for each model are presented in figure10. All the models under-predicted the maximum load except d56- 0.004, d56-0.005 and d52-0.005. Though d52-0.004, d46-0.005-0.1 and d46-0.005 gave a minimum error of 5.35, 5.26 and 2.19% respectively, the load vs. deflection graph for d46-0.005 is the desired trend as it has a clear definition of maximum load.

The mode of failure can be predicted by observing the shear and the normal stress contours in the post-processing step. Figures 11-12 represent the shear and normal stress contours at maximum load respectively. It is observed that shear stress contours are more dominant across the wall diagonal than normal stress contours indication a shear failure. Concrete crushing and tensile stress concentrations are observed in figure 12 which are observed in the experiment.

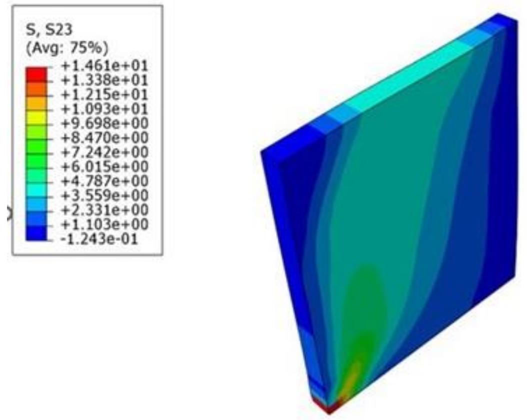

Figure 11 Shear stress component at maximum load for d46-0.005

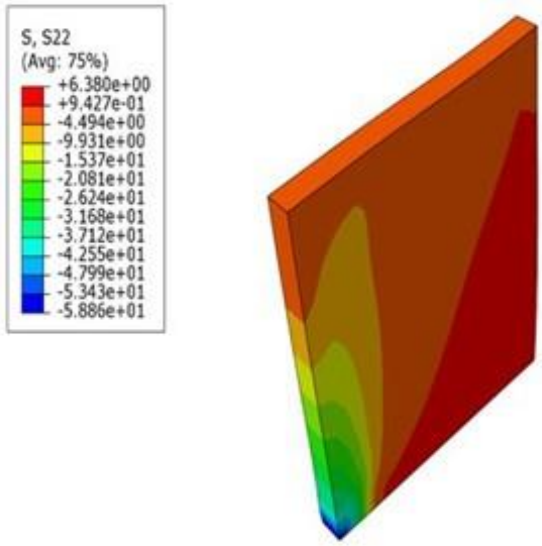

Figure 12 Normal stress components at maximum load for d46-0.005

5. CONCLUSIONS

The following conclusions can be drawn from the analytical study:

1. The viscosity parameter is directly related to the maximum predicted load. The higher the viscosity parameter, the slower are the plastic deformation and damage growth. The maximum load increases from 182.5 to 380.6kN as the viscosity parameter changes from 5E − 5 to 0.005 for dilation angle 56^{o}, as the viscosity changes from 0.001 to 0.005 for a dilation angle of 52^{o} the load increases from 221.4 to 357.9kN, and 304 to 334.5kN as the viscosity parameter changes from 0.004 to 0.005. Thus, viscosity parameter needs to be selected as it highly influences the maximum load to avoid erroneous results.
2. The finite element models are sensitive to the dilation angle as it affects the stress-strain response of concrete. The maximum load increases from 334.5 to 380.6kN as the dilation angle increases from 46^{o} to 56^{o}.
3. There is no significant effect of eccentricity on strength as the increase in the load when eccentricity changes from 0.1 to 1.0 is 3%.
4. As the stress contours can be captured continuously at each increment, FE models could capture the failure mode.
5. None of the models could predict the post-peak behavior where softening is expected to occur due to stiffness degradation. Thus, the static general solver does not predict the post-peak softening behavior.
6. In all the models the slope of the load vs. deflection response is rising compared to the experimental. Thus, stiffness of the finite element models is higher, and it could not capture the actual stiffness.
7. The dilation angle of 46^{o} in combination with the viscosity parameter of 0.005 and eccentricity e_c of 1.0 improve the results for shear wall failing in diagonal tension.

REFERENCES

[1] Andrés F Ocampo-Escobar and Aidcer L Vidot-Vega. Effects of concrete parameters in the lateral stiffness of reinforced concrete squat walls. *International Journal of Advanced Structural Engg*, 11:321–330, 2019.

[2] Thomas Paulay and MJ Nigel Priestley. *Seismic design of RC and masonry buildings*, v. 768. Wiley NY, 1992.

[3] Tevfik Terzioglu, Kutay Orakcal, and Leonardo M Massone. Cyclic lateral load behavior of squat RC walls. *Engg Structures*, 160:147– 160, 2018.

[4] Siamak Epackachi, Nikhil Sharma, Andrew Whitaker, Ronald O Hamburger, and Ayse Hortacsu. A cyclic backbone curve for squat RC shear walls. 2018.

[5] Pedro A Hidalgo, Christian A Ledezma, and Rodrigo M Jordan. Seismic behavior of squat RC shear walls. *Eq Spectra*, 18(2), 287–308, 2002.

[6] Buddhi Wahalathantri, David Thambiratnam, Tommy Chan, and Sabrina Fawzia. A material model for flexural crack simulation in reinforced concrete elements using abaqus. In *Proceedings of the first international conference on engineering, designing and developing the built environment for sustainable wellbeing*, pages 260–264. Queensland Univ of Technology, 2011.

[7] Mojtaba Labibzadeh, Alireza Firouzi, and Hamid R Ghafouri. Structural performance evaluation of an aged structure using a modified plasticity model in inverse solution method. *Inverse Problems in Science and Engineering*, 26(9):1326–1355, 2018.

[8] Adil M Mahdi. Impact of failure-surface parameters of concrete damage

plasticity model on the behavior of RUHPC beams. *Periodica Polytechnica Civil Engg*, 67(2):495–504, 2023.

[9] M Rasoolinejad and Zdeněk P Bažant. Size effect of squat shear walls extrapolated by microplane model m7. *ACI Strl Jl*, 116(3):75–84, 2019.

[10] V V Cao and Hamid R Ronagh. A model for damage analysis of concrete. *Ad in con conn*, 1(2):187, 2013.

[11] Abdeldjelil Belarbi, LX Zhang, and THOMAS TC Hsu. Constitutive laws of reinforced concrete membrane elements. In *Sociedad Mexicana deingenieria sismica in world conference on Eq Engg*, pp 1–8, 1996.

[12] Z H Marzoq and T M Borhan. Modelling hybrid reactive powder concrete t-beams, *Jl of Phy: Con Series*, 1895, 012054. IOP Pub, 2021.

[13] Barbara De Nicolo, Luisa Pani, and E Pozzo. Strain of concrete at peak compressive stress for a wide range of compressive strengths. *Materials and Structures*, 27:206–210, 1994.

[14] MR Behbahanifard, GY Grondin, and AE Elwi. Analysis of steel plate shear wall using explicit finite element method, *Proc. 13th WC. Eq Eng*, 2004.

[15] Shaohua Chen and Toshimi Kabeyasawa. Average stress-strain relationship of steel bars embedded in concrete. In *XIII World Conference on Earthquake Engg. Vancouver*, 2004.

[16] Jonas Enzell, Adrian Ulfberg, Gabriel Sas, and Richard Malm. Post-peak behavior of concrete dams based on nonlinear finite element analyses. *Eng Failure Analysis*, 130:105778, 2021.

[17] Rajbanshi, S., Kumar, A., & Dasgupta, K. Influence of CDP Parameters on Nonlinear Behaviour Of Slender RC Shear Wall With Enlarged BE. *17th WC on Eq Engg, 17WCEE*, Japan – Sep. 13-18 2020.